Calibration of a Photometric Cloud Condensation Nucleus Counter Designed for Deployment on a Balloon Package

D. J. DELENE* AND T. DESHLER

Department of Atmospheric Sciences, University of Wyoming, Laramie, Wyoming

ABSTRACT

The importance of atmospheric aerosols in understanding global climate changes has renewed interest in measurements of cloud condensation nuclei (CCN). To obtain high-resolution (125 m) vertical profiles of CCN number concentration, a balloon-borne instrument was developed. The instrument deduces the CCN concentration from measurements of laser light scattered by water droplets that condense on CCN within a static thermal-gradient diffusion chamber. The amount of light scattering is linearly proportional to the number of droplets within the diffusion chamber. Correlating the number of droplets within the sample volume with the amount of light scattered by the droplets provides the calibration constant that relates scattered light to CCN concentration. The calibration was tested by comparisons between the CCN counter and a condensation nuclei counter when sampling monodisperse aerosol larger than the CCN counter's critical activation size. The calibration constant depends on supersaturation, and depends slightly on the size of CCN that activate to form droplets. For dry NaCl aerosol between 35 and 160 nm, the calibration constant varies by less than 10% at 1% supersaturation. Calibration on ambient atmospheric aerosol is similar to calibration on laboratory-generated polydisperse NaCl aerosol, which indicates that the laboratory calibration can be applied to field measurements. During field and laboratory measurements, the time required for the activation and growth of droplets within the diffusion chamber is similar. Overall, the uncertainty of the calibration constant for the balloon-borne CCN counter is approximately 10% at 1% supersaturation.

1. Introduction

Cloud condensation nuclei (CCN) have a major influence on the cloud droplet number concentration and, hence, on the radiative properties of clouds. Increases in CCN concentrations, resulting from increased SO_2 emissions, have been suggested as a mechanism that could modify clouds properties sufficiently to affect global climate (Wigley 1989; Twomey 1991). The indirect effect of CCN on climate has started to be incorporated into global climate models (Meehl et al. 1996; Chuang et al. 1997; Pan et al. 1998). Pan et al. (1998) concluded from comparisons of climate models that refining input parameters might be more important than improving models to minimize uncertainties. CCN measurements are an important link in relating changes in aerosol concentration to changes in cloud droplet

number concentration (Boucher and Lohmann 1995; Liu et al. 1996). A balloon-borne CCN counter has been developed to provide vertical CCN profiles having a resolution of approximately 125 m. Since measurements obtained with the CCN counter are to be related to concurrent aerosol measurements instead of used simply to monitor changes in CCN concentration, an accurate calibration of the CCN counter is critical. The main objective herein is to describe the calibration of the balloon-borne CCN counter and its influence on the accuracy of field measurements.

The balloon-borne CCN counter described herein is similar to other static thermal-gradient diffusion chamber instruments (Radke and Hobbs 1969; Lala and Jiusto 1977; Bartlett and Ayers 1981; Hoppel and Wojciechowski 1981; Lala 1981). It uses a 670-nm solid-state laser to illuminate the center of the chamber, where the supersaturation is held at a prescribed value. To keep the instrument lightweight, a photodetector—instead of a photographic or charged coupled device (CCD) camera—is used to measure the CCN concentration. The photodetector voltage relates the amount of scattered light to the CCN concentration through the calibration constant for the instrument.

To obtain a CCN measurement at a single supersaturation requires 30 s. At the start of a measurement, the

* Current affiliation: Cooperative Institute for Research in Environmental Sciences, University of Colorado/National Oceanic and Atmospheric Administration, Boulder, Colorado.

Corresponding author address: David J. Delene, NOAA Climate Monitoring and Diagnostics Laboratory, R/E/CG1 325 Broadway, Boulder, CO 80303.
E-mail: ddelene@cmdl.noaa.gov

bottom-plate temperature is calculated based on the top-plate temperature and the desired supersaturation. The top-plate temperature is allowed to float with the enclosed temperature of the CCN counter. The bottom-plate temperature is controlled using thermoelectric coolers to achieve a prescribed supersaturation. The temperature difference between the top and the bottom plate is checked for 5 s to ensure that it is within the prescribed range ($\pm 0.2°$C). The chamber is flushed for 5 s to remove air from previous sample. A new air sample is captured and held within the chamber for 20 s. When a new air sample enters the chamber, CCN activate and droplets form, grow, and fall out.

Following the suggestion of Katz and Mirabel (1975), the temperature and the vapor pressure between the top and bottom plates are assumed to be linear functions of the height above the bottom plate. Both the top and bottom plates are kept wet for up to 3 h using saturated blotter papers. Delene et al. (1998) provided an initial description of the balloon-borne CCN counter, described calibration at 1% supersaturation on NaCl aerosols, and presented some preliminary CCN profiles. The focus herein is on dependence of the instrument's calibration on supersaturation, aerosol size, and aerosol type.

2. Standard calibration procedure

Calibration of the CCN counter is accomplished using Delene et al.'s (1998) method. The CCN concentration is equated to the number of water droplets in a measured portion of the laser beam, which are counted using a video camera and personal computer (PC) frame-grabber card. Concurrent with the video counts, the photodetector voltage is measured. A least squares linear fit between the photodetector voltage and the droplet count determines the calibration slope. The calibration constant for the CCN counter is defined as the calibration slope divided by the video sample volume. This study's calibration differs from that of Delene et al. (1998) in that it was performed employing a newer model video camera that has higher resolution, greater magnification, lower noise, and greater light sensitivity than the model used by Delene et al. (1998). The newer video camera is able to count more droplets within a 10-mm segment of the laser beam than the older model video camera can. Inquiries made to the laser manufacturer during this study indicate that the cross section of the laser beam is 5 mm $\times$ 1.8 mm, instead of the 4 mm $\times$ 1 mm used by Delene et al. (1998). Measuring the laser's cross section is uncertain because of laser beam blooming on the measurement apparatus. Our measurements of the laser beam width give 5.5 $\pm$ 0.5 mm, which compares favorably with the laser manufacturer's width of 5.0 mm. Although the newer model video camera counts more droplets, a larger sample volume is used, which results in a reduction of the calibration constant by approximately 18% compared with the calibration constant determined with the older video camera.

The gain setting of the PC frame-grabber card is used to test the sensitivity of the video camera. The number of droplets counted with the newer video camera does not increase with gain increases on the frame-grabber card. In contrast, the number of droplets counted with the older video camera does increase with gain increases on the frame-grabber card. Therefore, the new camera seems sensitive enough to count all droplets within the field of view of the laser beam without overcounting because of video noise.

Correctly setting the video camera's lens focus is critical for accurate calibrations. However, it is difficult to set the lens focus so that the entire depth of the laser beam is within focus. The focus of the lens is set by focusing on hairs of a Q-Tip placed within the video sample volume. The focus is checked periodically during calibration by examining the video camera's output on a monitor to ensure that no out-of-focus droplets (large droplets with dim centers) are present. The laser beam is at a 45° angle with respect to the lens, and the sample length along the laser beam is 10 mm. Thus, the depth of field needs to be 14 mm. This is significantly larger than the 5 mm width of the laser beam. In an attempt to decrease the sensitivity of the focus adjustment, the focal length was increased, which increases the depth of field but reduces the magnification of droplets. Increasing from 46 to 52 mm the distance from the center of the chamber to the lens results in an approximate 10% decrease of the 1% supersaturation calibration constant. The reduced magnification that results from this small increase in length probably resulted in undercounting because some droplets were now too small to be detected. For all calibrations presented herein, the lens was placed at 46 mm from the center of the chamber to give the greatest magnification of droplets possible, and the lens focus was set carefully to ensure that all droplets within the video sample were within focus.

Standard calibration of the CCN counter consists in obtaining several hundred comparisons of photodetector voltage and droplet concentration using laboratory aerosol produced from an ultrasonic vaporizer using a solution of 0.1 g L^{-1} of NaCl. The aerosol concentration is varied during a measurement sequence by changing the amount of filtered air mixed with the generated aerosol. Figure 1 presents an example of calibration data using the standard calibration method. The number of droplets at the time of the photodetector voltage peak and the video sample volume are used to determine the CCN concentration. The voltage peak method—instead of the voltage summation method of Delene et al. (1998)—is used here because the resulting calibration constants are similar and it simplifies examination of the calibration dependence on supersaturation.

3. Testing the standard calibration procedure

The video counting of droplets in the CCN chamber and, hence, the CCN calibrations, can be checked by
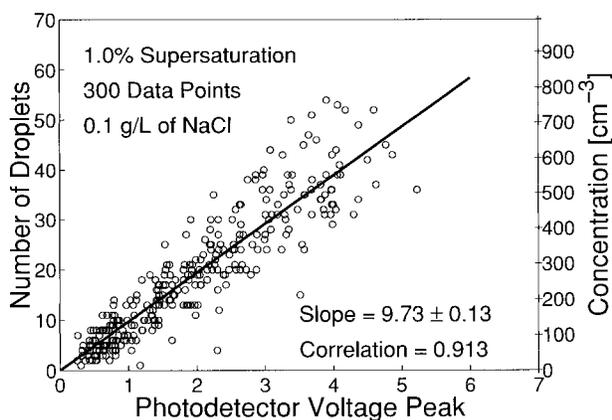
FIG. 1. The photodetector voltage peak versus the number of droplets counted within the video sample volume and the corresponding droplet concentration. Droplets are counted at the time of the photodetector voltage peak. The droplets nucleated on polydisperse NaCl aerosols produced using a solution of 0.1 g L^{-1} of NaCl in an ultrasonic vaporizer. The calibration slope (solid line) is the least squares linear fit to the data with a forced zero y intercept.

comparing the CCN concentration against measurements made by a Model 3010 TSI condensation nuclei (CN) counter, when sampling monodisperse aerosol larger than the CCN counter's critical activation size. The Model 3010 TSI CN counter is a good instrument with which to compare the CCN counter, since its detection efficiency is greater than 0.999 and its systematic error due to coincidence is less than 2% for aerosols larger than 30 nm in diameter and concentrations less than 3000 cm^{-3} (Mertes et al. 1995). Monodisperse aerosol of selected sizes is produced by atomizing an NaCl solution and passing the aerosol through a diffusion drier and a differential mobility analyzer (DMA; Knutson and Whitby 1975) into a conductive bag that is filled partially with filtered air. Sampling directly from the DMA was avoided because the counters could possibly affect the flow rates of the DMA and, hence, the aerosol size distribution. Once the conductive bag is filled, the CCN and CN counters sample concurrently from it. During sampling, the aerosol concentration decreases because of wall losses. Coagulation of aerosols within the bag is less than 2% for the concentrations (<1000 cm^{-3}) and times (<4 h) of the laboratory comparisons (Willeke and Baron 1993). Therefore, the size of the aerosols within the bag is considered to remain constant throughout the laboratory tests.

Figure 2 presents an example of the CCN and CN counters measuring 120-nm monodisperse NaCl aerosol. The CCN concentration is determined using the video camera to count droplets, at the time of the photodetector voltage peak, over a predetermined video sample volume. Below a concentration of 500 cm^{-3}, the averaged CCN concentrations agree with the CN concentrations. Above a concentration of 500 cm^{-3}, the CCN concentrations are low compared with the CN concentrations. The low CCN concentrations may be the
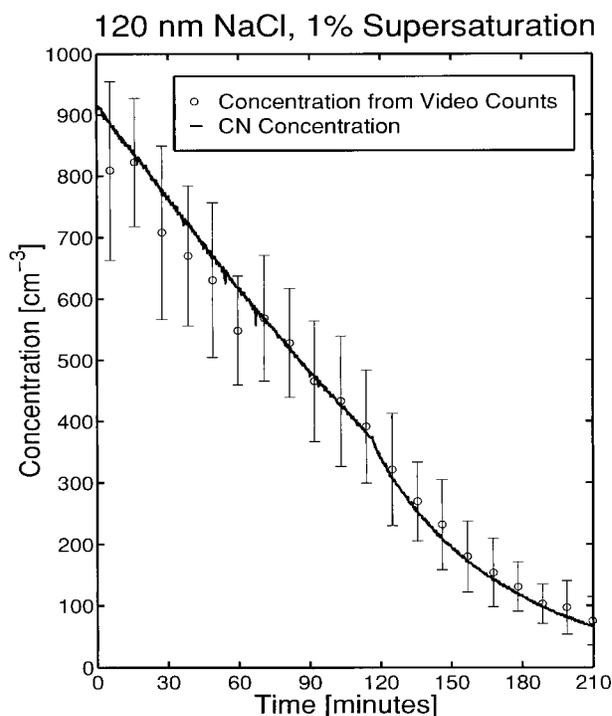

FIG. 2. Measurements of the concentration of 120-nm monodisperse NaCl aerosols using the CCN counter at 1% supersaturation (circles) and CN counter (solid line). The CCN concentration is measured using the video camera to count droplets over a predetermined video sample volume. The CCN concentration is averaged over approximately 20 samples (10 min), with the standard deviation given by the error bars. The decrease in concentration with time is the result of aerosol being removed to the walls of the sampling bag. Filtered air was added continuously to the sampling bag after 115 min.

result of undercounting droplets due to droplet coincidence within the viewing volume of the video camera. For the 3.5 h required to generate Fig. 2, the CCN counter was run continuously without rewetting the saturated blotter papers, which indicates that the saturated blotter papers on the top and bottom plates will remain moist for more than 3 h—the duration of a balloon flight.

4. Calibration dependence on supersaturation

The condensation growth rate of droplets is proportional to supersaturation. Therefore, at higher supersaturations, droplets will obtain sizes large enough to fall in a shorter amount of time. This is confirmed by observations of droplets within our thermal-gradient diffusion chamber. Changes in droplet size will affect the calibration slope since the amount of scattered laser light is proportional not only to droplet number but also to droplet size. Figure 3 illustrates the dependence of the calibration slope on supersaturation, which is fitted following the method of de Oliveira and Vali (1995). The increase in the calibration slope as the supersaturation decreases indicates that droplets decrease in size as the
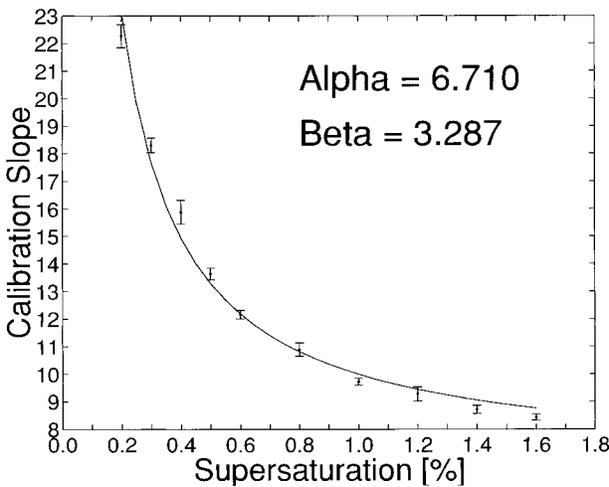
FIG. 3. The CCN counter's calibration slope dependence on su-persaturation. The data are fitted using the equation, $C =$ Alpha $+$ Beta/SS, in which Alpha and Beta are calibration constants, SS is the chamber supersaturation, and C is the calibration slope. Error bars represent one standard deviation in the calculated calibration slope.

supersaturation decreases and that the effect of this de-crease on scattering is not linear.

The droplet size dependence on supersaturation is ap-parent in the time dependence of the ratio of droplet number, or photodetector voltage, to the maximum drop-let number, or photodetector voltage. Figure 4 shows averages of these ratios over hundreds of samples as the CCN counter's chamber is flushed (first 5 s) and droplets activate, grow, and fall out. Ratio averages never equal 1, since the peak ratio does not always occur at the same time for each sample. The peak in droplet number (solid lines) occurs before the peak in photodetector voltage (dashed lines). This indicates that droplets continue to grow larger, and hence scatter more light, after the oc-currence of the droplet number peak. Averages of the ratios at 1% supersaturation, compared with 0.3% su-persaturation, have peaks that occur earlier in the mea-surement cycle and are narrower by a factor of 2. This difference is due to the droplet size dependence on su-persaturation that results from the supersaturation de-pendence of the condensation growth rate of droplets. Broad peaks in the averages of the ratios of the droplet number indicate that it does not make a significant dif-ference exactly where the count of the droplet number peak is obtained. However, with narrow peaks in the droplet number, it may be more important. This may be the reason that in Fig. 3 the data points, when compared with the data fit, show a slight (approximately 5%) un-dercounting at high supersaturations and a slight (ap-proximately 5%) overcounting at lower supersatura-tions.

Figure 5 illustrates the time required to reach the droplet number and photodetector voltage peaks as a function of supersaturation. The standard deviation of the average time to reach the photodetector voltage peak
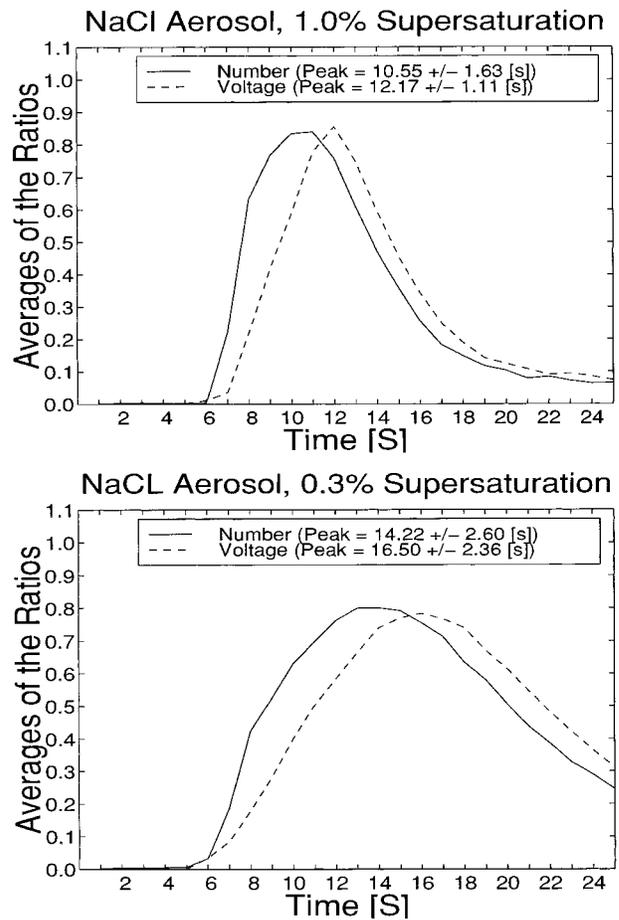

FIG. 4. Time versus the averages of ratios of droplet number (dashed line) and photodetector voltage (solid line) to the maximum number and voltage observed during the sample. The legends give the average and standard deviation times for the peak number of droplets and peak photodetector voltage. Time zero is at the beginning of a 5-s chamber flush. Following the chamber flush, an air sample is captured within the chamber; CCN activate; and droplets form, grow, and begin to fall.

increases with decreasing supersaturation. The increase in the variability in time to reach the peaks is due to broader peaks at lower supersaturation (Fig. 4). The time between the average droplet number peak and the av-erage photodetector voltage peak decreases linearly from 2.5 s at 0.3% supersaturation to 1.0 s at 1.6% supersaturation (Fig. 5). This further illustrates the de-pendence of condensation growth rate on supersatura-tion. Droplets grow more quickly at higher supersatu-rations, reducing the time between the droplet number and photodetector voltage peak.

5. Calibration dependence on aerosol type

The size distribution and chemical composition of atmospheric aerosols is highly variable in space and time because of the complex interrelationships between many different sources and sinks (Singh 1995). Although the
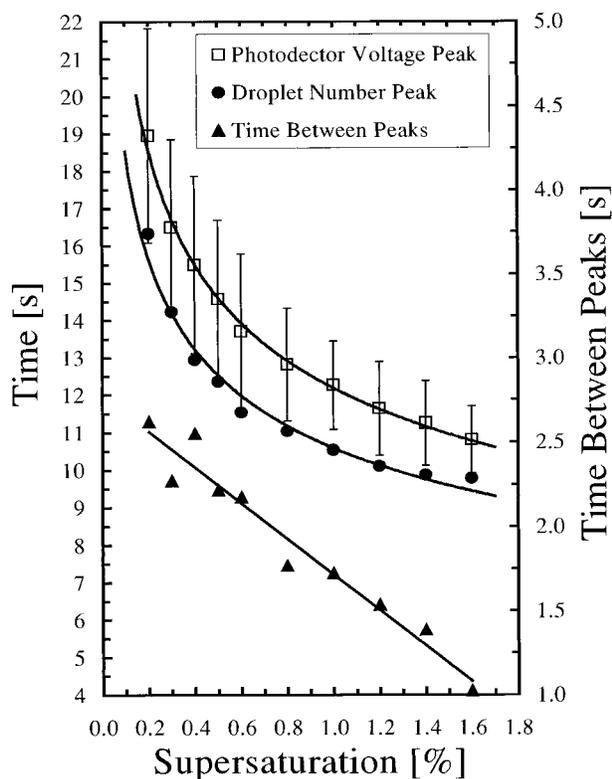
FIG. 5. Supersaturation of the CCN counter versus the average time to reach the number or voltage peak. The error bars on the photo-detector voltage time are one standard deviation of the average. Error bars (not shown) on the average time to reach the droplet number peak are similar. The left axis and solid triangles denote the time between the droplet number peak and photodetector voltage peak.

FIG. 6. Examples of the aerosol size spectrum generated using a solution of 0.1 g L^{-1} of NaCl in an ultrasonic vaporizer. The legend gives the total number concentration (cm^{-3}) for each aerosol size spectrum.

laboratory-generated calibration aerosol has a bimodal, polydisperse size spectrum, it consists of totally soluble aerosols, and the size distribution does not vary significantly from sample to sample. Thus, the calibration aerosols are different from ambient atmospheric aero-
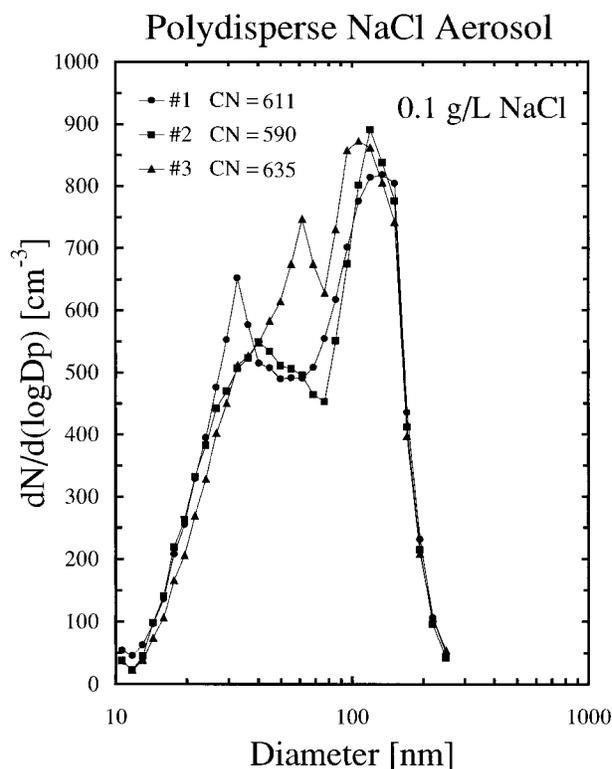
sols. Figure 6 presents representative aerosol size spectra for the NaCl laboratory-generated aerosols produced with the vaporizer. The aerosol spectra are obtained using a DMA and CN counter (Birmili et al. 1997).

To determine how the laboratory calibration is related to field measurements, the CCN counter was calibrated using different aerosol types. Table 1 summarizes sev-

TABLE 1. Calibration of the balloon-borne CCN counter at 1% supersaturation. The first column gives the calibration aerosol type: laboratory-produced aerosol using a solution of 0.1 g L^{-1} NaCl in a vaporizer, monodisperse NaCl aerosol of different diameters, or aerosol from the ambient atmosphere outside the laboratory building. The second column gives the calibration slope using the photodetector voltage peak. The third column gives the calibration slope using a three-point sum around the photodetector voltage peak (Delene et al. 1998). The fourth column gives the average time to reach the number peak in seconds from the beginning of the sample. The last column gives the average time to reach the voltage peak in seconds from the beginning of the sample. The first three rows give the results of the standard calibration of the CCN counter in Mar, Jun, and Oct 1998. The CCN counter was removed from the laboratory calibration bench between each standard calibration of the CCN counter and was used elsewhere. The calibrations presented in rows 3–10 were performed using the same focus and video camera alignment with the CCN counter.

Aerosol type	Peak method	Summation method	Droplet peak	Voltage peak
0.1 g L^{-1} NaCl	9.44 ± 0.09	3.57 ± 0.03	10.6 ± 1.7 (s)	12.5 ± 1.5 (s)
0.1 g L^{-1} NaCl	10.08 ± 0.08	3.78 ± 0.02	10.5 ± 1.9 (s)	12.4 ± 1.4 (s)
0.1 g L^{-1} NaCl	9.73 ± 0.13	3.64 ± 0.03	10.6 ± 1.6 (s)	12.2 ± 1.1 (s)
35 nm	10.20 ± 0.18	3.94 ± 0.05	10.2 ± 1.2 (s)	12.1 ± 1.1 (s)
50 nm	9.84 ± 0.11	3.66 ± 0.03	10.5 ± 1.5 (s)	12.6 ± 1.1 (s)
60 nm	9.60 ± 0.13	3.55 ± 0.04	10.7 ± 1.5 (s)	12.5 ± 1.2 (s)
80 nm	9.21 ± 0.12	3.40 ± 0.03	10.5 ± 1.4 (s)	12.4 ± 1.2 (s)
120 nm	9.09 ± 0.08	3.39 ± 0.02	10.8 ± 1.7 (s)	12.5 ± 1.4 (s)
160 nm	9.12 ± 0.09	3.37 ± 0.03	10.4 ± 1.6 (s)	12.2 ± 1.2 (s)
Outside	9.85 ± 0.10	3.72 ± 0.03	10.4 ± 1.7 (s)	12.2 ± 1.4 (s)

eral different calibrations of the CCN counter. The first three rows give the calibration results for three calibrations using the standard polydisperse NaCl aerosol: row 1 results are from March 1998, row 2 results are from June 1998, and row 3 results are from October 1998. No changes in the configuration of the CCN counter were made between these calibrations. However, the CCN counter was removed from the laboratory calibration bench between each of these calibrations and used elsewhere. The random errors of the calculated calibration slopes are given by the standard deviations in columns 2 and 3. The change in the calibration slopes (columns 2 and 3) for the standard calibration method (rows 1–3) is larger than the random errors for any one calibration. Systematic differences in the setup and alignment of the CCN counter with the video calibration system are believed to cause the variability between calibrations. The observed variability in the standard calibration method (rows 1–3) indicates that the calibration is repeatable to within 10%.

Roberts et al. (1997) observed a photodetector calibration dependence on the initial size of CCN in a static thermal-gradient diffusion chamber. To check for a calibration dependence on CCN size, the instrument was calibrated using monodisperse aerosol of several different sizes. The generation and sampling of the monodisperse aerosol was described earlier. Results of calibrations on different monodisperse aerosol sizes are given in rows 4–9 of Table 1. Aerosol size appears to have no detectable effect on the time to reach either the droplet number peak or the photodetector voltage peak (columns 4 and 5). However, an approximate 10% change in the calibration slope is observed between 35-nm and 120/160-nm NaCl aerosol. Further analysis of the measurements shows that there is no dependence between the time to reach the peaks and the aerosol concentration.

The calibration slope dependence on aerosol size indicates that the CCN size affects droplet size at the time of the photodetector voltage peak. This droplet size dependence on initial CCN size is not intuitive. Droplets are a few micrometers in diameter at the photodetector voltage peak based on their fall velocities. Since the diffusional droplet growth rate is proportional to the inverse of droplet radius, the droplet size spectrum becomes narrower as droplets grow to larger sizes (Howell 1949). Intuitively, the narrowing of the droplet spectrum is expected to cause the droplets to be at approximately the same relative size at the photodetector voltage peak. Therefore, the calibration should not depend on the initial CCN size.

Given the dependence of the calibration on CCN size, the calibration may change if we calibrate using atmospheric aerosol instead of laboratory-generated aerosol (Fig. 6). Figure 7 shows calibration data using ambient atmospheric aerosols obtained from outside the laboratory building on three consecutive mornings in early October in Laramie, Wyoming. The measurements
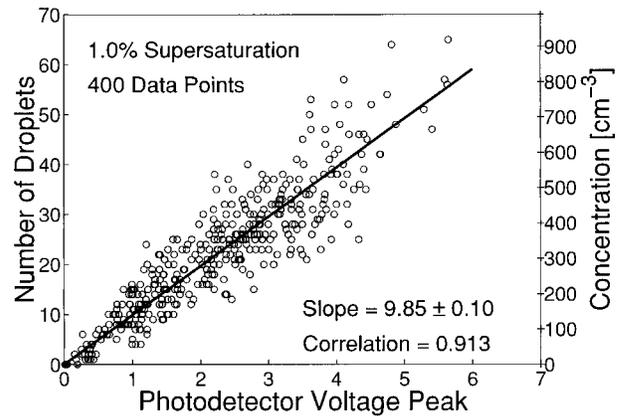

FIG. 7. CCN counter calibration data using aerosol from the ambient atmosphere outside the laboratory building in Laramie. The photodetector voltage peak versus the number of droplets counted within the video sample volume and the corresponding droplet concentration are shown. Droplets are counted at the time of the photodetector voltage peak. The calibration slope (solid line) is the least squares linear fit to the data with a forced zero y intercept.

were made at approximately sunrise under meteorological conditions of clear skies and high pressure—similar to a typical balloon flight. The ambient aerosol concentration was varied by diluting the aerosol sample with filtered air. Calibration on outside aerosol does not show a significant difference from the laboratory-generated NaCl aerosol. The calibration slope obtained using the outside air is within the range of slopes obtained for the three different calibrations on polydisperse laboratory aerosol (Table 1, rows 1–3). Furthermore, the average time to reach the peak values (Table 1, columns 4 and 5) and the shape of the average ratio peaks (not shown) are consistent with calibration on standard laboratory-generated aerosol. The consistency between the calibration on laboratory-generated aerosol and atmospheric aerosol measured at the surface in Laramie suggests that the laboratory calibration can be applied to field measurements.

It is unknown if atmospheric aerosols in the upper troposphere or at different geographic locations are different enough to invalidate the calibration. Although it is impossible to check the calibration on all types of aerosols, the average time to reach the photodetector voltage peak may indicate measurements that are not consistent with the laboratory calibration. Table 2 gives the time to reach the photodetector voltage peak for various field measurements. The surface and lower-tropospheric time to reach the photodetector voltage peak are consistent with the laboratory calibrations (Table 1). The upper-tropospheric time to reach the photodetector voltage peak shows more variability than the laboratory calibration data but is still within the range of the laboratory calibrations. The increase in variability in the upper troposphere may be related to measurements being near the detection limit of the CCN counter. The peak is less well defined near the detection limit, since

TABLE 2. Time to reach the photodetector voltage peak for field measurements in Laramie, Wyoming (41°N), Lauder, New Zealand (45°S); and Fairbanks, Alaska (65°N). Because of a clear difference in aerosol concentration, the field measurements are divided into summer and winter seasons. The third column gives the average and standard deviation of the time to reach the photodetector voltage peak. The fourth column gives the number of samples used to compute the average.

Layer	Location	Season	Voltage peak	Samples
Surface	Laramie	Summer	12.2 ± 1.4 (s)	400
Surface	Fairbanks	Winter	12.7 ± 1.8 (s)	144
Lower troposphere	Laramie	Summer	12.5 ± 1.1 (s)	86
Lower troposphere	Laramie	Winter	12.3 ± 1.0 (s)	18
Lower troposphere	Lauder	Summer	12.4 ± 0.7 (s)	23
Upper troposphere	Laramie	Summer	11.8 ± 1.6 (s)	117
Upper troposphere	Laramie	Winter	13.1 ± 2.7 (s)	68
Upper troposphere	Lauder	Summer	12.1 ± 1.3 (s)	67

only a few particles are within the photodetector sample volume.

6. Calibration error

Accurate CCN measurements require accurate droplet concentrations from the scattered light signal and knowledge of the supersaturation within the thermal-gradient diffusion chamber. The supersaturation within the chamber depends on the temperature difference between the top and bottom plates. Measurements with a thermocouple placed on the top and the bottom saturated blotter papers, within the thermal-gradient diffusion chamber, confirm that the temperature difference is maintained to within $\pm 0.1°C$ or $\pm 0.05\%$ supersaturation at a supersaturation of 1%. The supersaturation within the diffusion chamber, however, could be incorrect because transient supersaturations occur before steady-state temperature and moisture gradients are established (Fitzgerald 1970; Saxena et al. 1970). To avoid transient supersaturations that exceed the steady-state peak value, it is advantageous to have air samples enter the diffusion chamber at the top-plate temperature with a low relative humidity (Fitzgerald 1970; Saxena et al. 1970). The balloon-borne CCN counter's top-plate temperature is allowed to float with the instrument enclosure temperature. Before an air sample enters the chamber, it travels though 5-mm inside diameter stainless steel tubing within the instrument enclosure for approximately 0.3 s. Heat transfer calculations show that the air sample equilibrates with the enclosure temperature of the CCN counter before entering the chamber. Heat produced by the electronics ensures that the enclosure temperature is higher (from approximately 3°C at the surface to 30°C or more in the upper troposphere) than the ambient air temperature. Therefore, air entering at the enclosure temperature of the CCN counter also ensures that the relative humidity of the air sample is lower than the ambient relative humidity. Since air samples enter the CCN chamber at the enclosure temperature, transient supersaturations above the steady-state peak values are believed not to occur within the chamber under field measurement conditions.

The relative error in CCN concentration can be computed using Poisson counting statistics (Horvath et al. 1990). The Poisson counting error can be significant at upper-tropospheric concentrations since there are very few particles present in the laser beam. The counting error is larger for counting droplets via video than counting them via photodetector because the photodetector sample volume is approximately twice the video sample volume. The photodetector sample volume of 0.16 cm^{-3}, determined by Delene et al (1998), was verified using measurements collected during laboratory calibrations on monodisperse aerosols. The Poisson counting error agrees with the standard deviation of 10-min averages of CCN concentration. Poisson counting statistics give a range of errors from 36% to 11% for CCN concentrations (at ambient pressure) of 50 to 500 cm^{-3}. The measurement threshold is approximately 20 cm^{-3}, which corresponds to three droplets being within the photodetector sample volume. Below this concentration, the photodetector peak is not discernible from the baseline photodetector voltage determined during the chamber flush at the beginning of the sample.

The agreement between the CCN counter and a laboratory standard, the commercially built Model 3010 TSI CN counter seen in Fig. 2, indicates a good absolute calibration of the CCN counter. It also indicates that the video sample volume is correct, and the video camera/lens system is adequate to calibrate the CCN counter at 1% supersaturation. The variability, approximately 5%–10%, between standard calibrations of the CCN counter (Table 1, rows 1–3), is thought to result from systematic differences in the setup and alignment of the CCN counter with the video calibration system. Counting droplets using the photodetector to measure the scatter light signal—instead of counting droplets with a video camera system—has a small dependence on aerosol size. This size dependence is approximately the same as the systematic error in the standard laboratory calibration. The calibration dependence on aerosol size does not seem to have a great effect in the real atmosphere, since calibration on real atmospheric aerosol produces a calibration similar to the standard laboratory calibrations.

Considering all calibration results presented here, the calibration constant relating photodetector voltage to CCN concentration for the standard laboratory calibra-

tion of the balloon-borne CCN counter is believed to have an accuracy of 10% at 1% supersaturation. The video calibration of the CCN counter appears to work at supersaturations down to 0.2%. The calibration slopes fit nicely to a power law function (Fig. 3) However, video counting of droplets is difficult at low supersaturation, because of the smaller droplets, and the dependence of the calibration constant on aerosol size may be more significant at lower supersaturations than at 1%. The video calibration method should be verified at low supersaturations.

7. Conclusions

A photometric CCN counter was calibrated using a video camera and PC frame-grabber card to count droplets. Droplet number is related linearly to the amount of laser light scattered by the droplets. The standard calibration procedure for the CCN counter is repeatable to better than 10% accuracy. The calibration relationship between droplet number and photodetector voltage was verified by a comparison between the CCN counter and a CN counter when sampling monodisperse aerosol. Calibration of the CCN counter is found to depend on supersaturation and to have a slight dependence on the size of CCN that activate to form droplets. The dependence on supersaturation is accounted for easily using a power law function to relate the calibration slope to supersaturation. The calibration dependence on CCN size is less than 10% at 1% supersaturation. Calibration on ambient atmospheric aerosol appears similar to the standard calibration procedure. Laboratory calibration measurements, compared with field measurements at various locations and within different atmospheric layers, give average photodetector voltage peaks that occur at similar times after an air sample enters the thermal-gradient diffusion chamber. Therefore, it appears that within the diffusion chamber atmospheric CCN behave similarly to laboratory-produced CCN. Random errors in measured CCN concentration can be computed using Poisson counting statistics, and range from 36% to 11% for CCN concentrations in the range of 50 to 500 cm^{-3}. The calibration constant that relates photodetector voltage to CCN concentration is believed to have an accuracy of 10% at 1% supersaturation.

REFERENCES

Bartlett, B. M., and G. P. Ayers, 1981: Static diffusion cloud chamber. *J. Rech. Atmos.,* **15,** 231–233.

Birmili, W., F. Stratmann, A. Wiedensohler, D. Covert, L. M. Russell, and O. Berg, 1997: Determination of differential mobility analyzer transfer functions using identical instruments in series. *Aerosol Sci. Technol.,* **27,** 215–223.

Boucher, O., and U. Lohmann, 1995: The sulfate-CCN-cloud albedo effect: A sensitivity study with two general circulation models. *Tellus,* **47B,** 281–300.

Chuang, C. C., J. E. Penner, K. E. Taylor, A. S. Grossman, and J. J. Walton, 1997: An assessment of the radiative effects of anthropogenic sulfate. *J. Geophys. Res.,* **102,** 3761–3778.

Delene, D. J., T. Deshler, P. Wechsler, and G. Vali, 1998: A balloon-borne cloud condensation nuclei counter. *J. Geophys. Res.,* **103,** 8927–8934.

de Oliveira, J. C. P., and G. Vali, 1995: Calibration of a photoelectric cloud condensation nucleus counter. *Atmos. Res.,* **38,** 237–248.

Fitzgerald, J. W., 1970: Non-steady-state supersaturations in thermal diffusion chambers. *J. Atmos. Sci.,* **27,** 70–72.

Hoppel, W. A., and T. A. Wojciechowski, 1981: Description and discussion of the NRL TGDCC. *J. Rech. Atmos.,* **15,** 209–213.

Horvath, H., R. L. Gunter, and S. W. Wilkison, 1990: Determination of the coarse mode of the atmospheric aerosol using data from a forward-scattering spectrometer probe. *Aerosol Sci. Tech.,* **12,** 964–980.

Howell, W. E., 1949: The growth of cloud drops in uniformly cooled air. *J. Meteor.,* **6,** 134–149.

Katz, J. L., and P. Mirabel, 1975: Calculation of supersaturation profiles in thermal diffusion cloud chambers. *J. Atmos. Sci.,* **32,** 646–652.

Knutson, E. O., and K. T. Whitby, 1975: Aerosol classification by electric mobility: Apparatus, theory, and applications. *J. Aerosol Sci.,* **6,** 443–451.

Lala, G. G., 1981: An automatic light scattering CCN counter. *J. Rech. Atmos.,* **15,** 259–262.

——, and J. E. Jiusto, 1977: An automatic light scattering CCN counter. *J. Appl. Meteor.,* **16,** 413–418.

Liu, P. S. K., W. R. Leaitch, C. M. Banic, and S. M. Li, 1996: Aerosol observations at Chebogue Point during the 1993 North Atlantic Regional Experiment: Relationships among cloud condensation nuclei, size distribution, and chemistry. *J. Geophys. Res.,* **101,** 28 971–28 990.

Meehl, G. A., W. M. Washington, D. J. Erickson III, B. P. Briegleb, and P. J. Jaumann, 1996: Climate change from increased CO_2 and direct and indirect effects of sulfate aerosols. *Geophys. Res. Lett.,* **23,** 3755–3758.

Mertes, S., F. Schroder, and A. Wiedensohler, 1995: The particle detection efficiency curve of the TSI-3010 CPC as a function of the temperature difference between saturator and condenser. *Aerosol Sci. Technol.,* **23,** 257–261.

Pan, W., M. A. Tatang, G. J. McRae, and R. G. Prinn, 1998: Uncertainty analysis of indirect radiative forcing by anthropogenic sulfate aerosols. *J. Geophys. Res.,* **103,** 3815–3823.

Pueschel, R. F, 1995: Atmospheric aerosols. *Atmospheric Aerosols: Composition, Chemistry, and Climate of the Atmosphere,* H. B. Singh, Ed., Van Nostrand Reinhold, 120–175.

Radke, L. F., and P. V. Hobbs, 1969: An automatic cloud condensation nuclei counter. *J. Appl. Meteor.,* **8,** 105–109.

Roberts, G., R. Flagan, G. Lala, and M. Andreae, 1997: Photodetector output calibration of a photometric static thermal-gradient cloud condensation nuclei counter. *16th Annual Conf. of the American Association for Aerosol Research,* Denver, CO, American Association of Aerosol Research, 439.

Saxena, V. K., J. N. Burford, and J. L. Kassner Jr., 1970: Operation of a thermal diffusion chamber for measurements on cloud condensation nuclei. *J. Atmos. Sci.,* **27,** 73–80.

Twomey, S., 1991: Aerosols, clouds, and radiation. *Atmos. Environ.,* **25A,** 2435–2442.

Wigley, T. M. L., 1989: Possible climate change due to SO_2-derived cloud condensation nuclei. *Nature,* **339,** 365–367.

Willeke, K., and P. A. Baron, 1993: *Aerosol Measurement: Principles, Techniques, and Applications.* Van Nostrand Reinhold, 876 pp.